Research Square

Preprints are preliminary reports that have not undergone peer review.
They should not be considered conclusive, used to inform clinical practice,
or referenced by the media as validated information.

Exploring the Potential of Phygital Bone as a Synthetic Surrogate for Forensic Bone Trauma

Victoria Rzymelka
Universitat Autònoma de Barcelona
Juan Crespo-Santiago
Elisava Barcelona School of Design and Engineering
Marco Gesualdo
Elisava Barcelona School of Design and Engineering
Anna Álvarez
Elisava Barcelona School of Design and Engineering
Clàudia Andreu
Elisava Barcelona School of Design and Engineering
Helena Mallafré
Elisava Barcelona School of Design and Engineering
Xavier Garrido
Mossos d'Esquadra
Nathalie Schwab
Institute of Legal Medicine St.Gallen
Marta Otero-Viñas
University of Vic - Central University of Catalonia (UVIC-UCC)
Ignasi Galtés
Catalonian Institute of Legal Medicine and Forensic Science (IMLCFC)
Xavier Jordana
xavier.jordana@uab.cat

Universitat Autònoma de Barcelona

Article

Keywords: Bone trauma, Synthetic bone surrogate, Forensic trauma reconstruction, Bone biomechanics, 3D-printed bone model

Posted Date: July 24th, 2026

DOI: https://doi.org/10.21203/rs.3.rs-10206802/v1

License: This work is licensed under a Creative Commons Attribution 4.0 International License.
Read Full License

Additional Declarations: Competing interest reported. J. Crespo-Santiago, X. Jordana, M. Gesualdo, I. Galtés and M. Otero-Viñas are inventors on a patent application (Application No. EP 24383123.7, filed on the 14th of October 2024) related to the design and use of the PHyB synthetic bone model evaluated in this study. This application is currently under review. All other authors declare no competing interests.

Abstract

Mechanical trauma analysis is vital in forensic investigations to determine causes of death, yet current synthetic bone surrogates inadequately replicate human bone's biomechanical and microstructural properties. Here we explore the potential of the Phygital Bone (PHyB) model, a 3D-printed synthetic femur reproducing human bone macro- and microarchitecture, against fresh human femora and commercial surrogates (Synbone, Sawbones) via compression, three-point bending, and gunshot trauma tests. PHyB closely matched human femora in compression stiffness and fracture patterns, while Sawbones better approximated bullet energy loss. None fully replicated bending behavior. Cortical trait analysis revealed PHyB shares some fracture characteristics with human bone, indicating improved biomimicry. These findings suggest PHyB offers a promising platform for forensic trauma reconstruction, particularly for compression-related scenarios, though further validation across diverse loading conditions is needed before widespread forensic application.

1. Introduction

Forensic anthropologists play a crucial role in medical-legal investigations of deaths as they asses the mechanisms of trauma in human skeletal remains or in bodies that have been subjected to taphonomic changes such as burning, saponification, scavenger activity or mummification [1, 2, 3]. In those cases, evaluation of the soft tissues is usually not possible so that the focus of investigation lays on the bones. They are more resistant and reliable in comparison to the soft tissue when exposed to taphonomical factors. For this reason, bones become a critical and permanent trauma evidence in forensic research and can aid in pointing the weapon used or in reconstructing the events leading to death [4, 5, 6].

In an experimental setting, trauma mechanisms can be investigated by comparing the injuries found on a victim with those inflicted on simulant materials, such as biological bones (human or animal) or synthetic bone models, that accurately represent the affected anatomical area [7]. Several studies already focused on comparing experimental data with real traumatic cases across these models. A study by Harden et al. [8] compared the effects of two dynamic loading rates on the fracture characteristics of human ribs during bending. Similarly, Weathley [9] investigated the differences between perimortem and postmortem fracture patterns in 76 deer femurs. A more recent study by Schwab et al. [10] analysed the variations in fracture patterns across deer, human, and synthetic bone models following gunshot trauma.

However, several challenges remain in identifying appropriate surrogate materials for bone trauma experiments, which can ultimately affect the accuracy of injury reconstruction studies. Because an in-depth understanding of injury mechanics and bone biomechanics is crucial to forensic science, forensic anthropologists have increasingly collaborated with biomechanical engineers to expand the existing knowledge and drive research in this area [11].

Materials that simulate human tissue, such as bone, are commonly used in empirical research such as ballistics or blunt force trauma (BFT) reconstruction [7]. Human tissue surrogates can be valuable in

reconstructing crime scene dynamics when sufficient evidence cannot be found [7]. Animal models for example have been used in experimental research for a long time due to the assumption that non-human and human models are similar [12]. Pigs are the golden standard as they are the ones that resemble humans the most anatomically [7]. Mostly their skulls and femurs are used. Nevertheless, porcine bones still are morphologically and biomechanically different and there is no animal that precisely resembles that of humans [10]. Even though Kieser et al. [13] found that compared to sheep and pig bones, deer femurs were the most similar to human femurs.

The use of human cadavers is also applied in research however, only after the deceased person specifically donated their body to science during lifetime. The lack of efficient donor programs, good cadaver transportation methods and ethical issues pose as a huge limitation on using human remains as experimental material [7]. Another limiting factor in using human specimens is thus the small sample size. The high variability regarding age, sex and pathology related changes such as osteoporosis or the state of the bone marrow and the lack of its standardisation poses another constraint in using human bones [14].

In order to avoid the ethical issues associated with performing experimental research on animal or human tissue, there is great interest in finding an alternative model that could produce ballistic or BFT fracture patterns of human long bones [10]. To address this problem researchers have started to create and apply computed-based models as well as biofidelic analogues [12]. In forensic anthropological research such as bone trauma reconstruction several existing analogues are already being applied.

Sawbones produced human bone proxies for medical research, practice and experimentation purpose [15]. A model that has been used in several validation studies is the Sawbones Model 3403, a representation of the human femur [16]. It is made of short fibre filled epoxy, filled with short glass fibres in order to simulate the cortical bone [17]. In a study by A. Khalil fracture patterning of Sawbones tibias were compared to fractures found in autopsy cases in a three-point bending test [18]. An agreement between both samples was found suggesting that Sawbones models could also be a potentially satisfactory substitute for human bones in forensic research [11].

Another company producing bone surrogates is Synbone which first developed polyurethane surrogates for surgical training [10]. Later they specialised in bone analogues for forensic experiments such as ballistic impacts on long bones. Their models have been used in several gunshot trauma experiments even though a study by Henwood & Appleby-Thomas [19] suggested a greater similarity in fracture patterning to porcine bones rather than human ones. Schwab et al. [10] performed comparative GST on Synbone femora (Model PR0108) and humeri (Model PR0109) as well as deer femora. Even though promising results were found, such as that deer and Synbone models produce similar fracture patterns, a range of differences were found too. Schwab et al. [10] suggest that caution needs to be prevailed when using those bone analogues and call for more comparative studies.

Nevertheless, while Sawbones and Synbone both produce synthetic bone analogues for surgical training and forensic research, their priority is to mimic the material properties of the cortical and cancellous

human bone rather than reconstructing the entire hierarchical microstructure.

Phygital Bone (PHyB) is an emerging solution developed by Crespo-Santiago et al. [20]. This collaboration brought together expertise from design, engineering, and forensic medicine to overcome this limitation by integrating advanced digital modelling and fabrication techniques. By focusing on creating a more accurate model of bone structure, PHyB aspires to replicate the complexity of human anatomy [20]. The promising model is biomimetic, and a full-scale representation of the human femur manufactured through stereolithography (SLA) 3D printing, it not only represents the macrostructure but also the microstructure of human bone at an osteonal level, imprinting lamellae and Haversian canals. The model is fully parametric due to is Algorithm Aided Design (AAD) and customizable to address patient-specific requirements [20].

Phygital Bone holds significant potential for forensic research; by replicating both the macro- and microstructure of natural bone, this synthetic model offers a high-fidelity platform for trauma analysis and forensic investigations.

This study aims to evaluate the validity of the PHyB model as a bone surrogate in trauma experiments by comparing it with fresh human femora and established commercial surrogates, such as Synbone and Sawbones. Mechanical and ballistic assessments, including compression tests, three-point bending tests, and gunshot trauma (GST) impact analysis, were conducted to compare these materials.

2. Material and Methods

2.1 Samples

The samples used in this study included fresh human femur bones and synthetic bone models from Synbone, Sawboness, and PHyB (Table 1). The PHyB model was manufactured with a Form4 (FormLabs) 3D printer with Rigid 4000 resin (FormLabs) according to Crespo-Santiago et al. [20]. The Synbone (PR0108.G) and Sawbones (3403-15) models were ordered through the manufacturer's websites.

The human bone samples used in this study were retrieved from adult males aged 45–65 years and were obtained from biological material originally collected for previous studies conducted by the Institute of Legal Medicine and Forensic Sciences of Catalonia (IMLCFC). The human femur (N = 7) and Synbone (N = 10) data used for the GST were retrieved from Schwab et al. [10].

This study was conducted in accordance with the Declaration of Helsinki (Fortaleza, Brazil, Oct 2013) and was approved by the local ethics committee (Bellvitge University Hospital, L'Hospitalet de Llobregat, Barcelona, Ref. PR416/20, 14/12/2020). Human bone samples were processed in line with the legal requirements of Spain (Law 14/2007, RD 1716/2011 and RD 9/2014) and guidance for clinical use (EEC regulations 2004/23/CE and 2006/17/CE). Human biological samples were obtained through the Donor Center–Barcelona Tissue Bank, which is responsible for donor recruitment, obtaining and safeguarding informed consent documentation, and ensuring compliance with all applicable ethical and legal

requirements. The samples used in this study are stored in the private collection at the IMLCFC in Barcelona, Spain (Registro Nacional de Biobancos. Ref. C.0004241).

Table 1
Description of the specimens including shaft diameter (mm), cortical thickness (mm), length (mm), and number of samples used per test (N). GST = Gunshot Trauma.

				Compresssion		Three-Point bending		GST	
Sample group	**Model**	**Shaft diameter (mm)**	**Cortical thickness (mm)**	**Length (mm)**	**N**	**Length (mm)**	**N**	**Length (mm)**	**N**
Human femur	**Fresh femur**	28.7 ± 0.29	5.79 ± 0.63	30	3	100	1	461.1 ± 3.18	7
Synbone	**PR0108.G**	30	5	30	3	100	4	270	10
Sawbones	**3403-15**	30	4.3	30	3	100	5	250	5
PHyB	**F4K**	30	6	30	6	100	5	200	5

2.2 Sample preparation

For the compression tests Synbone (n = 3), Sawbones (n = 3), fresh femur (n = 3) and PHyB F4K (n = 6) samples were prepared, each 30 mm long. To create those samples each specimen was cut at a speed of 22,000 rpm with a Komet Dental saw (0.20 mm) that was attached to a N-120 Navfram machine (Mod. 6250). To avoid any measurement errors while the samples were being compressed, and to make them as parallel as possible each end of the samples was polished with an Metaserv 2000 grinder (Buehler) at a speed of 250 rotations using a Buehler SiC Grinding Paper for metallography (wet or dry, P600). For the three-point bending tests Synbone (n = 4), Sawbones (n = 5), fresh femur (n = 1), and PHyB F4K (n = 5) samples were prepared, each 100mm long. The samples were cut with the same method as the compression test samples. Polishing the transversal surface was not needed in this case as the specimens were placed horizontally on the pedals thus the transversal surface was not in direct contact with the pedals. For the GST experiment, Synbone (n = 10), Sawbones (n = 5), fresh femur (n = 7), and PHyB F4K (n = 5) samples were used.

2.3 Biomechanical and Trauma Experiments

2.3.1 Compression and Three-Point Bending Tests

All mechanical tests were performed with a ZwickRoell Retroline 1475 universal testing machine (ZwickRoell) equipped with a 50 kN load cell. Data were acquired with the machine software TestExpert v.III 1.7 (ZwickRoell) at a sampling rate of 500 Hz. Two loading configurations were employed: uniaxial compression and three-point bending. For compression assays, specimens were placed between parallel steel platens; surfaces were prepared to ensure flat, parallel contact faces to minimize eccentric loading.

No lubrication was applied and contact conditions were assumed to be consistent across all specimens. For flexural testing, the machine was equipped with a standardized three-point bending fixture. All tests were conducted at a constant crosshead displacement of 2.5 mm/min until failure.

The elastic modulus (E) was determined from the linear region of the stress-strain curve using the automatic regression function of TestExpert v.III 1.7 (ZwickRoell) applied over a strain range beginning 0.5%. Strain was determined by normalizing crosshead displacement to the initial specimen height, while peak stress was defined as the maximum recorded stress prior to failure. Uniaxial compression was selected to characterize compressive stiffness and strength under controlled boundary conditions, enabling direct benchmarking of PHyB specimens against fresh femoral samples and commercial surrogates. Three-point bending was selected as a standardized configuration to assess flexural behavior under comparable geometry constraints.

2.3.2 Gunshot Trauma

The GST was performed in collaboration with the Mossos d'Esquadra, Catalan Police at the Ballistic Unit (Laboratoris de Policia Cientifica, Divisió de Policia Científica dels Mossos d'Esquadra). The experiments using Synbone and fresh femur sample were done in a previous study by Schwab et al. [10]. For the Sawbones and PHyB F4K samples, we followed the same procedure for the GST experiment. Prior to shooting all samples were embedded in ballistic gelatine blocks with a diameter of 10 cm and a thickness before the target of 2cm according to a study by Bir et al. [21]. (Clear Ballistics Gel®). Each specimen was placed in an upright position and held by a self-constructed stabilization device. Samples were positioned 2 m from the muzzle (Fig. 1) of a 9 mm Luger test barrel (Drello Bal 1025 FU-R) [10].

The impact velocity of the shot projectile was 360 m/s which simulates a handgun shot. To shoot the sample in the middle each sample was marked with a permanent marker, and an optical laser was pointed at it. A NonTox 9.00 mm Luger full metal jacket projectile from Sellier&Bellot was used with a mass of 7.98 g. The exit velocity of the projectile upon impact was measured with the use of a light barrier (Drello LS 11 – 03) and its computerised system (Drello VC 4043-09). The bullets' post impact velocity was used to calculate the kinetic energy (Ke = 0.5 mv2) lost in each group where the bullet mass (m) is 7.98g and (v) the exit velocity of the bullet after target penetration (Energy loss (J) = impact energy – exit energy).

2.4 Cortical Trait Analysis

The cortical traits of the GST samples were analysed following the framework established by Schwab et al. [10] which entails a characterisation of ballistic fracture patterns in human long bones. To reconstruct the cortical traits in the shot samples the fragments of each specimen were collected and reassembled using a transparent, water resistant, universal glue (Imedio). The fractures were examined macroscopically, and cortical traits were divided into entrance, exit and general features (Table 2).

Table 2

List of the cortical traits used for macroscopic examination of the samples following Schwab et al. [10]. The traits are divided into entrance, exit and general trait.

Entrance traits	
Round hole	The bullets initial entry defect that visually appears round.
V-shape	Describes the shape of the bone proximal/distal to the entry hole. The tip of the v-shape points towards the bullet entry. The margins of the v-shape are built by oblique fracture lines
Y-branching	Is present proximal and/or distal of the entry hole. It is a bifurcation of the longitudinal fracture line into two oblique lines that run toward both lateral aspects.
Tip fragmentation	A superficial, external loss of cortical fragment(s) at the tip of the bone around the entry hole. It only appears proximal/distal of the bullet entry. Typically, chiselled edges indicate a sharply defined transition to the intact cortical bone. In case oblique fractures separate the bone, tip fragmentation on bone parts next to each other creates the image of a stepped circular margin around the bullet entry
Wing flake	A loose trapezoidal flake of cortical bone resembling spread wings. The aspect facing the entry hole features part of the ring defect. In contrast to tip fragmentation, it comes from the lateral aspect(s) of the entry hole. It may be broken and thus incomplete
Wing flake defect	The superficial cortical defect on the lateral aspect(s) of the entry hole that is produced when the wing flake breaks out
Ring defect	A circular or partial circular loss of superficial cortical bone on the entry hole's margin. Its presentation reminds of an abrasion ring. It can be interrupted by other entrance traits such as tip fragmentation
Internal beveling	A funnel shape in the cortical wall with a larger extent on the internal side
Radiating fracture lines	Longitudinal, transversal or oblique fractures that radiate away from the entry hole
Exit traits	
Round hole	The bullets exit defect that visually appears round.
Square hole	The bullets exit defect that visually appears edgy or square.
Layered breakage	Is a layered pattern visible on the fracture surface
External beveling	A funnel shape in the cortical wall with a larger extent on the external side
Radiating fracture lines	Transversal, longitudinal or oblique fractures that radiate away from the exit hole
General traits	

Entrance traits	
Plastic deformation	Is the persistent deformation of bone
Wall splitting	A separation of bone within the cortical wall

2.5 Data Analysis

Mechanical testing results from compression and three-point bending experiments were visualised using box plots to compare variation across different sample groups. For GST analysis qualitative and quantitative data were assessed. Qualitative data were analysed using contingency tables (Fisher's exact test) and multiple correspondence analysis to identify patterns and associations. A One-Way ANOVA test was done for the bullet energy loss to see if there are differences between groups, followed by the Levene's Homogeneity test and a Tukey's Post Hoc test to find out which groups differ significantly from each other. Values below 0.05 were stated as significant ($p < 0.05$).

3. Results

3.1 Compression Tests

The mechanical performance of synthetic and biological femoral models was evaluated through comparative compression tests. Parameters including elastic modulus, fracture force, maximum stress, and displacement at maximum force were analyzed to assess differences in stiffness, strength, and deformation behavior among the samples. Descriptive statistics (Table 3) were calculated for each variable to summarize the central tendency and variability of the measured mechanical properties.

Table 3

Descriptive statistics of mechanical properties across sample groups. Values are presented as mean ± standard deviation (SD).

Sample Group	**N**	**Elastic Modulus E (GPa)**	**Fracture Force (N)**	**Maximum Stress (MPa)**	**dL at Fmax (mm)**
		Mean ± SD	***Mean ± SD***	***Mean ± SD***	***Mean ± SD***
Fresh Femur	3	3.30 ± 1.37	39673 ± 26.547	101 ± 17.2	1.83 ± 0.666
Synbone	3	1.14 ± 0.089	4293 ± 214	55.5 ± 1.75	10.6 ± 0.299
Sawbones	3	3.16 ± 0.598	9943 ± 136	123 ± 7.50	1.27 ± 0.153
F4K	6	3.50 ± 0.191	55000 ± 0.00	120 ± 0.005	5.02 ± 1.83

The compression test results are presented in the box plots below (Fig. 2).

Among the tested models, the PHyB F4K model most closely matched the fresh femur specimens in terms of stiffness (Young's modulus) and failure load (fracture force). The Sawbones model also performed well in stiffness and deformation. In terms of deformation, the F4K model was similar to the fresh femur but showed some variability. Overall, both F4K and Sawbones were the most similar to the fresh femur mechanical properties under the present compression configuration

3.2 Three-Point Bending Tests

The mechanical performance of synthetic and biological femoral models was evaluated through three-point bending tests. Parameters including elastic modulus, fracture force, maximum force, and displacement at maximum force were analyzed to assess differences in stiffness, strength, and deformation behavior among the samples. Descriptive statistics (Table 4) were calculated for each variable to summarize the central tendency and variability of the measured mechanical properties.

Table 4

Descriptive statistics of mechanical properties across sample groups. Values are presented as mean ± standard deviation (SD).

Sample Group	N	Elastic Modulus E (GPa)	Fracture Force (N)	Maximum Force (N)	dL at Fmax (mm)
		Mean ± SD	***Mean ± SD***	***Mean ± SD***	***Mean ± SD***
Fresh Femur	1	0.356 ± —	3186 ± —	3262 ± —	1.09 ± —
Synbone	4	0.194 ± 0.044	4907 ± 488	4989 ± 520	5.84 ± 3.09
Sawbones	5	1.58 ± 0.270	4625 ± 672	4972 ± 233	2.18 ± 0.00
F4K	5	0.489 ± 0.007	4554 ± 1,014	4689 ± 1,102	3.37 ± 1.68

The three-point bending test results are presented in the box plots below (Fig. 3).

Overall, no synthetic bone model matched the fresh femur across all parameters. However, the F4K model most closely approximated its stiffness, fracture force, and maximum force, while Sawbones was most similar in displacement behavior and exhibited a brittle failure pattern comparable to that of human femur bone.

3.2 Cortical Trait Analysis

To investigate differences in trauma expression after ballistic impact across Sawbones, Synbone, PHyB F4K and real human femur qualitative cortical traits following Schwab et al. [10] were analysed. The results offer an understanding into the extent to which synthetic bone models replicate trauma patterns observed in real human cortical bone.

Table 5

Descriptive statistics of ballistic cortical traits across sample groups. Sample size (N). Trait occurrence (%). Fisher's exact test p-value: *p < 0.05, **p < 0.01, ***p < 0.001.

Entrance traits	**Human Femur (N = 7) %**	**F4K (N = 5) %**	**Synbone (N = 10) %**	**Sawbone (N = 5) %**	**p-value**
Round hole	100	40	100	100	**
V-shape	100	40	40	80	*
Y-branching	0	60	70	0	**
Tip fragmentation	86	100	60	0	**
Wing flake	57	0	0	60	**
Wing flake defect	86	0	0	40	***
Ring defect	100	0	0	100	***
Internal beveling	100	0	100	100	***
Radiating fracture lines	100	100	100	100	
Exit traits					
Round hole	14	0	20	100	**
Square hole	86	20	80	0	**
Layered breakage	100	100	0	0	***
External beveling	100	100	90	100	
Radiating fracture lines	100	100	100	100	
General traits					
Plastic deformation	100	0	0	0	***
Wall splitting	29	20	90	0	**

All cortical traits except radiating fracture lines and external bevelling show significant differences between sample groups in trait occurrence after ballistic impact (Table 5). Synbone is strongly associated with the occurrence of wall splitting and Y-branching. Sawbones is closely associated with round exit holes, suggesting it tends to produce cleaner and more uniform penetration channels. The PHyB F4K models is associated with tip fragmentation and layered breakage. The human femur is linked to plastic deformation, wing flake, wing flake defect and ring defect, traits that are linked with deformation irregularities, most probably due to biomechanical properties of real bone tissue (Fig. 4).

3.3 Projectile Energy Dissipation

The initial kinetic energy of the bullet was 517.1 Joules (J). The absolute energy loss of the bullet varied between samples, indicating differences in their ballistic resistance. Data for Synbone and the human femur were taken from Schwab et al. [10].

The human femur exhibited the highest median energy loss of 352J (SD = 29.86) (Fig. 5). Sawboness showed the most similar energy loss to the human femur with an absolute loss of 314 J (SD = 8.18). The PHyB F4K model followed with a median energy loss of 257 J (SD = 15.05). In contrast, the Synbone model demonstrated the lowest energy absorption with a mean of 169J (SD = 10.71), indicating less resistance to projectile impact. The observed variability highlights notable differences in biomechanical behaviour between human and synthetic bone surrogates

The PHyB and Sawbones models more closely resemble the energy-absorbing behavior of real human bone compared to the Synbone variant. One-way ANOVA analysis demonstrated significant differences ($p < 0.001$) between groups, suggesting that none of the synthetic bone models accurately represent the biomechanical behavior of a human femur. Homogeneity of variance was tested using Levene's test and was not violated ($p = 0.110$).

4. Discussion

This study aimed to validate the Phygital Bone model by evaluating its performance against fresh human femur bones and available synthetic bone surrogates, specifically Synbone (PR0108.G) and Sawbones (3403-15), within the context of forensic trauma research. The objective was to determine whether PHyB offers a more accurate representation of human femoral trauma characteristics and mechanical behaviour than current commercial alternatives Synbone and Sawbones. For this purpose, the study integrated standardized mechanical testing (compression and three-point bending), with ballistic experiments involving gunshot trauma (GST). Furthermore, qualitative and quantitative fracture assessments were performed utilizing the criteria established by Schwab et al. [10] for ballistic fracture analysis. Altogether, this multifaceted approach facilitated a comprehensive evaluation of the PHyB model’s utility and its potential for integration into forensic research.

Mechanical behaviour of PHyB vs. Human femur vs. Synbone vs. Sawbones

Compression

Compression test results demonstrated that the PHyB F4K and Sawbones models most closely approximate the mechanical behaviour of the fresh human femora regarding stiffness, failure load, and deformation. Both models demonstrated a significantly higher correlation to human femur than the Synbone model.

Because PHyB F4K and Sawbones exhibit biofidelity under compressive loading, they may provide a useful simulation for trauma reconstruction, particularly in scenarios involving blunt force trauma or high-energy impacts.

Three-Point bending

Results from the three-point bending tests showed that Synbone exhibited an exceptionally high deformation of 7 mm at peak force, rendering it an unrealistic surrogate for human femur. While Sawbones surpassed the fresh femur in stiffness and strength, it maintained a comparable displacement rate. Although the PHyB F4K exceeded the fresh femur across all measured parameters, it demonstrated the closest overall mechanical profile compared to Synbone and Sawbones.

Consequently, while no synthetic model perfectly replicated the mechanical performance of the fresh femur, the PHyB F4K demonstrated the closest overall mechanical profile among the tested surrogates for three-point bending applications.

Bullet energy loss

The findings of the bullet energy loss after ballistic impact showed that Sawbones and PHyB F4K absorbed more kinetic energy than Synbone which demonstrated a limited resistance to ballistic impact. Among the tested synthetic bone surrogates, Sawbones exhibited the highest median energy loss of 314 J (SD = 8.18) and was the closest to the human femur which had a median energy loss of 352 J (SD = 29.86). The PHyB F4K model was close to Sawbones with a median loss of 257 J (SD = 15.05). The differences between the synthetic bone models and the human femur suggest that material composition and structural design play a crucial role in the response to ballistic trauma. The superior performance of Sawbones might be due to its denser materials and fibre composition which resembles the fibre composition and structure of real bone. This is consistent with the review by Petre & Leeuwenburgh [22] that underlines the fact that the main advantage of fibres used in biomaterials for tissue engineering is the improvement of the biomechanical performance. The above-mentioned results are also consistent with the findings of Schwab et al. [10], who reported a higher ballistic resistance in bone compared to Synbone. Nonetheless, the statistical results demonstrated significant differences between all compared bone models suggesting that no synthetic bone model fully replicates the ballistic response seen in human femur bones.

Cortical Trait Analysis

The multiple correspondence analysis revealed that different synthetic bone models exhibit unique clustering based on cortical trauma features. Synbone was strongly associated with wall splitting and y-branching which is indicative of a brittle fracture response and a simplified structure. Both cortical traits have been previously observed in the study by Schwab et al. [10]. Sawbones was associated with a round exit hole which suggest an easier passage of the projectile. Those results might be explained by the uniform density and low heterogeneity of the synthetic bone surrogates compared to real bone. The human femur was associated with plastic deformation, ring defect and a wing flake defect, indicating a more complex stress distribution. Those findings are supported as well by Schwab et al. [10] where at least ring defect and wing flake defect were found to be distinct for human bone. Importantly, the PHyB F4K model shows similarity to the human femur in terms of its layered breakage pattern. This suggests

that the PHyB F4K model shares some characteristics with real human bone, such as the layered breakage pattern observed after ballistic impact. However, wall splitting and square exit hole are specific for Synbone and PHyB F4K. Those differences might be due to material properties, manufacturing processes or structural differences in those models.

Limitations

Despite the promising performance of the PHyB model, several limitations of this study should be acknowledged.

Small sample constraints

The relatively small sample size per experimental group limits the statistical power of the findings, particularly for the fresh femur sample (N = 1) in the three-point bending tests. While the observed trends provide a clear indication of material behavior, further testing with larger sample sizes is necessary to verify these results and to strengthen the overall conclusions.

Ballistic variability

The gun shot trauma experiments were restricted to a single projectile type. Because variations in projectile caliber and composition generate variable energy transfer dynamics, the resulting fracture patterns and energy loss profiles may differ significantly under varied ballistic conditions. Consequently, these results represent an initial insight into high-energy impact behavior rather than a comprehensive characterization of all ballistic variables.

5. Conclusions

This study aimed to explore the validity of the Phygital Bone model for forensic research by comparing its performance against established synthetic surrogates Synbone and Sawbones, and fresh human femur. The objective was to determine if PHyB could more accurately replicate the mechanical and trauma-related characteristics of biological bone than commercial surrogates. Following a combination of mechanical testing (compression and three-point bending), gunshot trauma analysis, and cortical trait assessment, the PHyB F4K model demonstrated a comparatively higher degree of biofidelity. While Synbone was found to lack sufficient structural and biomechanical realism, Sawbones provided a credible ballistic response. However, the PHyB F4K model showed some similarity in mechanical properties to human bone and demonstrated aspects of improved performance in ballistic impact response and fracture patterning. Hence, it may offer a promising surrogate for trauma reconstruction in forensic casework and biomechanical research. Beyond the F4K variant specifically, Phygital Bone represents a significant advancement in biomimetic bone modelling by successfully reproducing essential microstructural elements such as osteons, lamellae, and cement lines. Although no synthetic model can yet fully replicate the inherent complexity of the human femur, these findings suggest that PHyB provides a more sophisticated and realistic alternative to existing commercial surrogates.

Nevertheless, despite this high performance, PHyB remains in the developmental phase. Further validation, reproducibility testing, and refinement are essential before this emerging model can be integrated into standardized forensic protocols or casework. Future research should focus on comparative fracture pattern analysis under blunt force trauma and three-point bending, utilizing the methodologies established by Scheirs et al. [23, 24] to expand the experimental database and further validate the Phygital Bone model.

Institutional Review Board Statement

This study was conducted in accordance with the Declaration of Helsinki (Fortaleza, Brazil, Oct 2013) and was approved by the local ethics committee (Bellvitge University Hospital, L'Hospitalet de Llobregat, Barcelona, Ref. PR416/20, 14/12/2020). All human bone samples were processed in line with the legal requirements of Spain (Law 14/2007, RD 1716/2011 and RD 9/2014) and guidance for clinical use (EEC regulations 2004/23/CE and 2006/17/CE). The samples are stored in the private collection at the IMLCFC in Barcelona, Spain (Registro Nacional de Biobancos. Ref. C.0004241). All human biological samples used in this study were obtained through the Donor Center–Barcelona Tissue Bank, which is responsible for donor recruitment, obtaining and safeguarding informed consent documentation, and ensuring compliance with all applicable ethical and legal requirements. Consequently, all donors provided informed consent for the donation and research use of their biological samples. The research team received the samples through the Tissue Bank's authorized procedures and did not have access to the donors' confidential consent records, which are securely maintained by the Tissue Bank in accordance with ethical standards and data protection regulations. Owing to the confidential nature of these records, individual informed consent forms cannot be disclosed or provided.

Declarations

Acknowledgements

The authors would like to thank the Central Unit of Ballistics and Instrumental Traces of Mossos d'Esquadra for gunshot trauma experiments; and Alan Wückert, Mario Fradera, Joan Ribot, David Grothe, Alex Olivella, Nim Carbonell, Maria J. de Pouplana and Gerard Estrada for their valuable contributions to the success of this research.

Funding

This research was funded by: AEI Clusters Spanish Ministry for Industry and Tourism (AEI-010500-2024-18), Llavor AGAUR Gencat (2023 LLAVOR 0005), and Proyectos de Generación de Conocimiento, Agencia Estatal de Investigación (PID2021-124112NB-100).

Conflict of Interest

J. Crespo-Santiago, X. Jordana, M. Gesualdo, I. Galtés and M. Otero-Viñas are inventors on a patent application (Application No. EP 24383123.7, filed on the 14th of October 2024) related to the design and use of the PHyB synthetic bone model evaluated in this study. This application is currently under review. All other authors declare no competing interests.

Author contributions statements

Victoria Rzymelka: Writing original draft, review & editing, Methodology, Investigation, Formal analysis, Data curation, Conceptualization. **Juan Crespo-Santiago**: Writing original draft, review & editing, Supervision, Project administration, Methodology, Investigation, Funding acquisition, Formal analysis, Data curation, Conceptualization. **Marco Gesualdo**: Visualization, Validation, Software, Methodology, Investigation, Data curation, Conceptualization. **Anna Álvarez**: Visualization, Validation, Software, Investigation, Data curation, Conceptualization. **Clàudia Andreu**: Validation, Investigation, Formal analysis, Data curation. **Helena Mallafré**: Visualization, Validation, Software, Investigation, Formal analysis, Conceptualization. **Xavier Garrido**: Methodology, Investigation, Conceptualization. Nathalie Schwab: Visualization, Validation, Investigation, Data curation, Conceptualization, Formal analysis. **Marta Otero-Viñas**: Writing review & editing, Supervision, Funding acquisition. **Ignasi Galtés**: Supervision, Writing review & editing, Resources, Methodology, Data curation, Conceptualization. **Xavier Jordana:** Writing original draft, review & editing, Supervision, Project administration, Methodology, Investigation, Funding acquisition, Formal analysis, Data curation, Conceptualization.

References

1. Byers, S. N. (2017). Introduction to forensic anthropology (5th ed.). Routledge.
2. Indra, L., Errickson, D., Young, A., & Lösch, S. (2022). Uncovering forensic taphonomic agents: Animal scavenging in the European context. Biology, 11(4), 601. https://doi.org/10.3390/biology11040601
3. Love, J. C., & Wiersema, J. M. (2016). Skeletal trauma: An anthropological review. Academic Forensic Pathology, 6(3), 463–477. https://doi.org/10.23907/2016.047
4. Haglund, W.D.; Sorg, M.H. Forensic Taphonomy: The Postmortem Fate of Human Remains; CRC Press: Boca Raton, FL, USA, 1997; ISBN 978-0-8493-9434-8.
5. Saukko, P.; Knight, B. Knight's Forensic Pathology, 3rd ed.; CRC Press: Boca Raton, FL, USA, 2004; ISBN 978-1-4441-1538-3.
6. Sexton, K., Schwab, N., Galtés, I., Casas, A., Armentano, N., Brillas, P., Garrido, X., & Jordana, X. (2024). Osteonal damage patterns from ballistic and blunt force trauma in human long bones. Life, 14(2), 220. https://doi.org/10.3390/life14020220
7. dos Santos, L. M. P., da Cunha, M. R., Reis, C. H. B., Buchaim, D. V., da Rosa, A. P. B., Tempest, L. M., da Cruz, J. A. P., Buchaim, R. L., & Issa, J. P. M. (2025). The use of human tissue surrogates in anatomical modeling for gunshot wounds simulations: An overview about "how to do" experimental terminal ballistics. Frontiers in Bioengineering and Biotechnology, 13, 1536423. https://doi.org/10.3389/fbioe.2025.1536423

8. Harden, A. L., Kang, Y.-S., & Agnew, A. M. (2022). Comparison of the effect of two dynamic loading rates on fracture characteristics of human ribs in bending: An experimental study. Forensic Anthropology, 5(4), 1–16. https://doi.org/10.5744/fa.2021.0028
9. Wheatley, B. P. (2008). Perimortem or postmortem bone fractures? An experimental study of fracture patterns in deer femora. Journal of Forensic Sciences, 53(1), 69–72. https://doi.org/10.1111/j.1556-4029.2008.00593.x
10. Schwab, N., Jordana, X., Soler, J., Garrido, X., Brillas, P., Savio, A., Lavín, S., Ortega-Sánchez, M., & Galtés, I. (2023). Can Synbone® cylinders and deer femurs reproduce ballistic fracture patterns observed in human long bones? Journal of Materials Science, 58(11), 4970–4986. https://doi.org/10.1007/s10853-023-08333-6
11. Antonelli, L. S. (2024). A biomechanical evaluation of nonhuman analogues in skeletal trauma research [Master's thesis, California State University, Chico].
12. Dempsey, N., & Blau, S. (2020). Evaluating the evidentiary value of the analysis of skeletal trauma in forensic research: A review of research and practice. Forensic Science International, 307, 110140. https://doi.org/10.1016/j.forsciint.2020.110140
13. Kieser, D. C., Kanade, S., Waddell, N. J., Kieser, J. A., Theis, J. C., & Swain, M. V. (2014). The deer femur—a morphological and biomechanical animal model of the human femur. Bio-Medical Materials and Engineering, 24(4), 1693–1703.
14. Beisekenov, N., Sadenova, M., Azamatov, B., & Syrnev, B. (2025). Analysis of Biomechanical Characteristics of Bone Tissues Using a Bayesian Neural Network: A Narrative Review. Journal of Functional Biomaterials, 16(5), 168. https://doi.org/10.3390/jfb16050168
15. Sawbones. (n.d.-a). About us. Retrieved March 8, 2025, from https://www.sawbones.com/about-us
16. Sawbones. (n.d.-b). Biomechanical test materials validation studies. Retrieved March 8, 2025, from https://www.sawbones.com/validation-studies
17. Sawbones. (n.d.-c). Top biomechanical products & materials provider for testing and validation. Retrieved March 8, 2025, from https://www.sawbones.com/biomechanical-product-info
18. Khalil, A. L. (2014). An analysis of the propagation of butterfly fractures in the lower limbs initiated through blunt force trauma [Master's thesis, California State University, Los Angeles].
19. Henwood, B. J., & Appleby-Thomas, G. (2020). The suitability of Synbone® as a tissue analogue in ballistic impacts. Journal of Materials Science, 55(7), 3022–3033.
20. Crespo-Santiago, J., Jordana, X., Gesualdo, M., Álvarez, A., Andreu, C., Mallafré, H., Rzymelka, V., Galtés, I., Otero-Viñas, M. (2026). Phygital bone: A biomimetic parametric model for 3D-printed synthetic human bone. Results in Engineering, 29, 109889. https://doi.org/10.1016/j.rineng.2026.109889
21. Bir, C., Andrecovich, C., DeMaio, M., & Dougherty, P. J. (2016). Evaluation of bone surrogates for indirect and direct ballistic fractures. Forensic Science International, 261, 1–7. https://doi.org/10.1016/j.forsciint.2016.01.023

22. Petre, D. G., & Leeuwenburgh, S. C. G. (2020). The use of fibers in bone tissue engineering. Tissue Engineering Part B: Reviews, 28(1), 141–159. https://doi.org/10.1089/ten.TEB.2020.0252
23. Scheirs, S., Malgosa, A., Sánchez-Molina, D., Ortega-Sánchez, M., Velázquez-Ameijide, J., Arregui-Dalmases, C., Medallo-Muñiz, J., & Galtés, I. (2017). New insights in the analysis of blunt force trauma in human bones: Preliminary results. International Journal of Legal Medicine, 131(3), 867–875. https://doi.org/10.1007/s00414-016-1514-1
24. Scheirs, S., Hevink, B., Ortega-Sánchez, M., Jordana, X., McGlynn, H., Rodriguez-Baeza, A., Malgosa, A., & Galtés, I. (2019). Intra vitam trauma pattern: Changing the paradigm of forensic anthropology? International Journal of Legal Medicine, 133(2), 661–668. https://doi.org/10.1007/s00414-018-1958-6

Figures

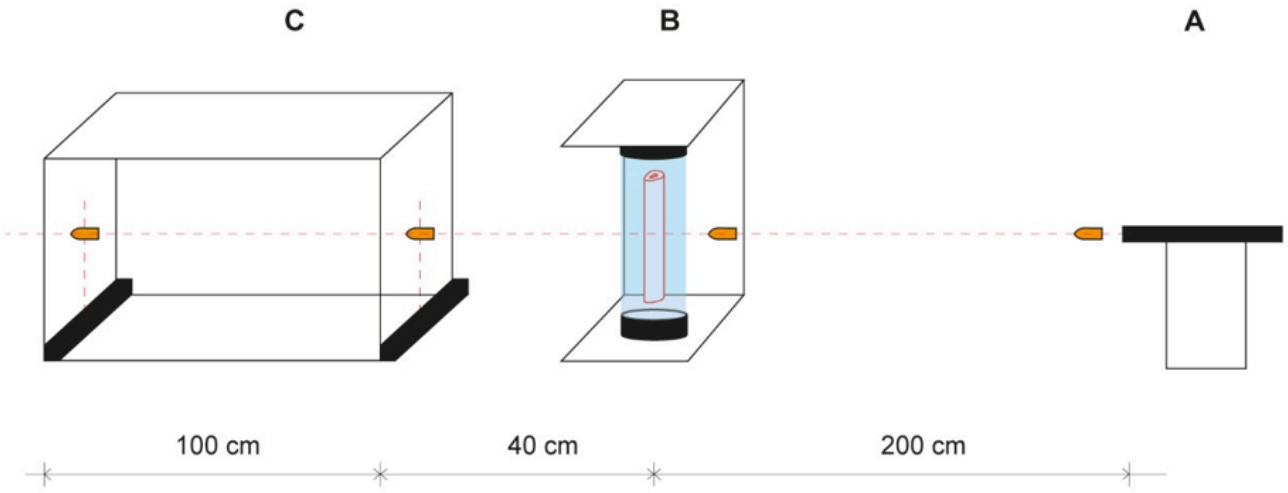


Figure 1

Experimental set up of the ballistic testing procedure. A) Barrel firing the bullet (orange), B) Table with metal stabilizers supporting the PHyB F4K sample embedded in ballistic gelatine (blue). C) Light sensors (black) used to measure the bullet trajectory and exit velocities (red dotted line).

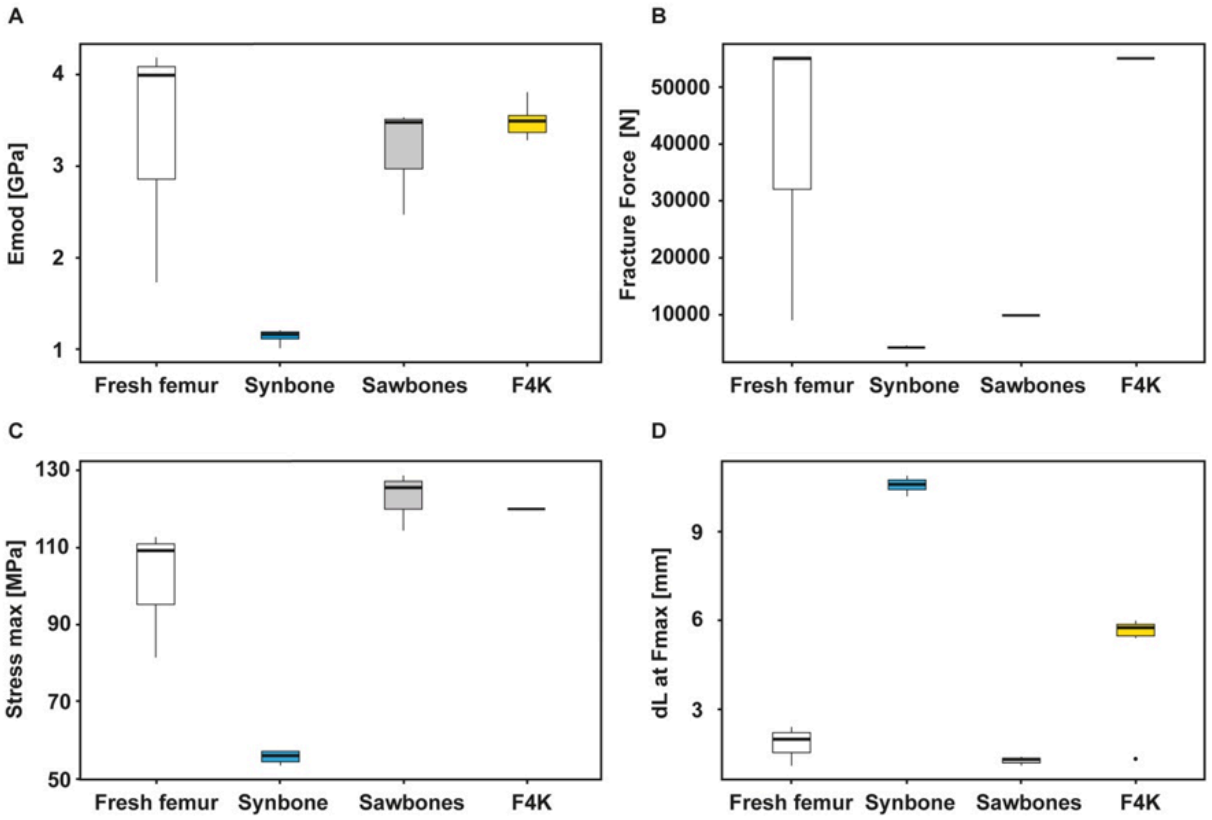


Figure 2

Compression test results. Comparison of the mechanical properties across synthetic bone models and fresh femur bones. Box plots show: (A) Young's modulus (GPa), (B) fracture force (N), (C) maximum stress (MPa), and (D) displacement at maximum force (mm). Boxes represent the interquartile range (IQR), central lines indicate the median, whiskers represent 1.5 x IQR data from first (Q1) and third (Q3) quartiles, and dots represent outliers.

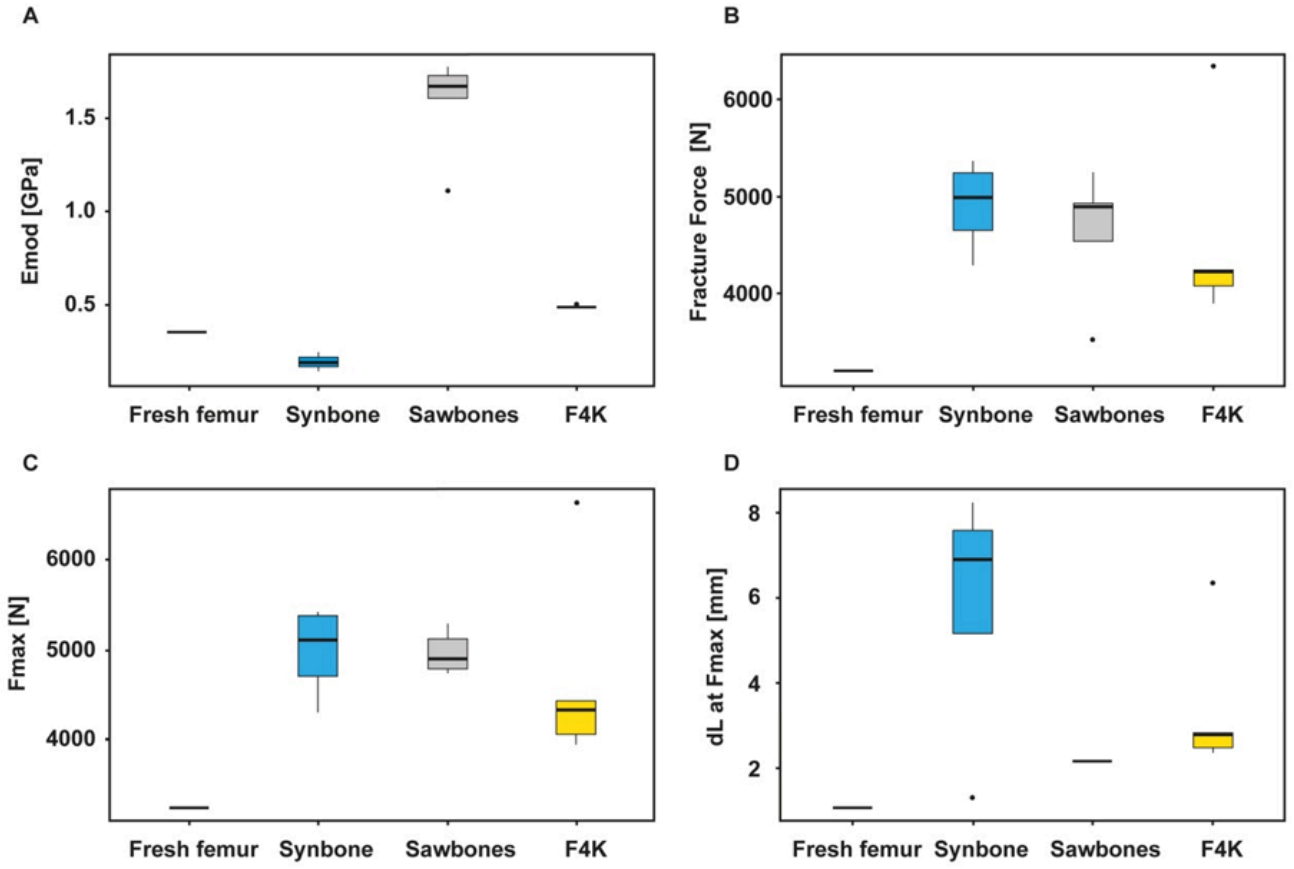


Figure 3

Three-point bending test results. Comparison of the mechanical properties of synthetic and biological bone materials. Box plots show: (A) Young's modulus (GPa), (B) fracture force (N), (C) maximum force (N) and (D) displacement at maximum force (mm). Boxes represent the interquartile range (IQR), central lines indicate the median, whiskers extend to 1.5 x IQR data from first (Q1) and third (Q3) quartiles, and dots represent outliers.

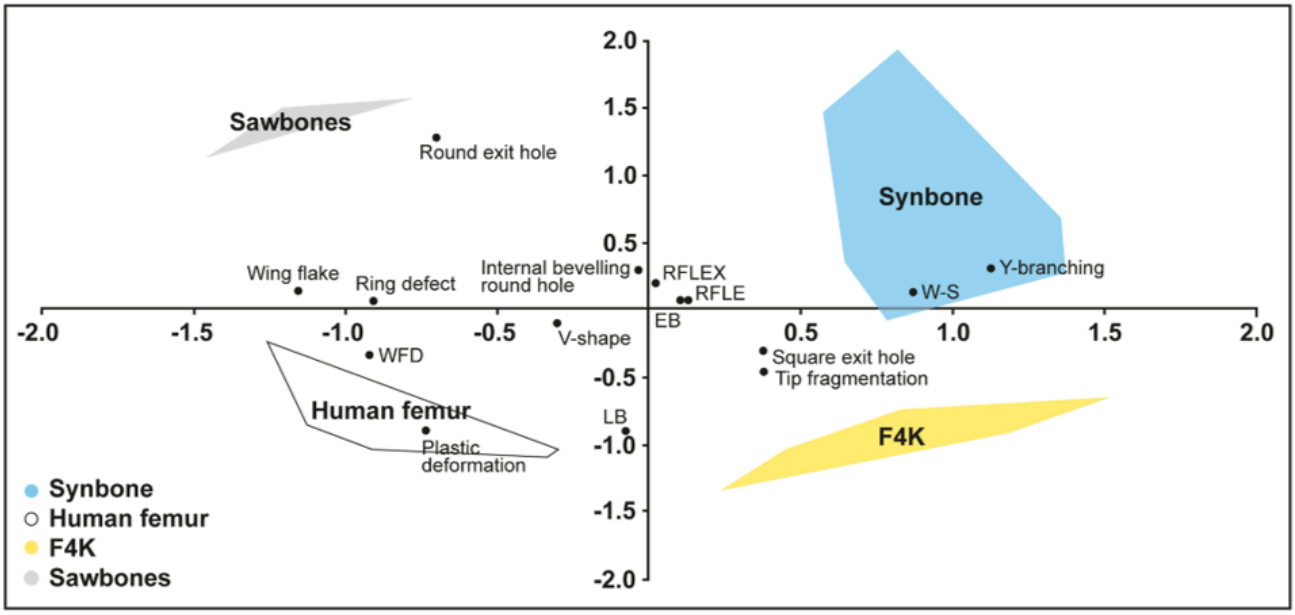


Figure 4

Correspondence analysis showing associations between bone surrogates and ballistic cortical traits. Proximity between variables indicates stronger relationships. Upper left = Sawbones, upper right = Synbone, lower left = human femur, and lower right = PHyB F4K. WFD = wing flake defect, EB = external bevelling, LB = layered breakage, WS = wall splitting, RFLE = radiating fracture lines at entry, RFLEX = radiating fractures lines at exit.



Figure 5

Box plot showing bullet energy loss in joules (J) across different bone models. The dot represents an outlier. Statistical significance is indicated as follows: *p<0.05, **p<0.01, ***p<0.001.

Supplementary Files

This is a list of supplementary files associated with this preprint. Click to download.

- Supplementarymaterial.docx